cult to describe the surface with discontinuities by a single patch using surface parametric coordinates. Simply dividing the surface into a number of local patches is ineffective, since there are grid cells extending over two side surfaces at the edges of the side surfaces of the pyramid. The present method, which can deal with plural patches, treats this problem easily. The effect of the weight function λ is seen in Fig. 3. The surface of $z = \sin x \sin y$ is examined. In Fig. 3c, $\lambda = \text{const}$; however, in Fig. 3d, λ is set to be proportional to the radius of the curvature. The clustering is performed successfully around the top of the curve without changing the point distribution on the boundary.

Summary

A new method of generating the surface grid has been presented. The capabilities of generating the smooth surface grids from the unstructured grid are demonstrated. An adaptive control of the mesh clustering is achieved by using the weight function. The accuracy of the surface definition is expected to improve further if the high-order patches are introduced.

Acknowledgments

The author deeply acknowledges S. Shirayama of the Institute of Computational Fluid Dynamics for his discussions. He is also grateful to J. M. Hyun of the Korea Advanced Institute of Science and Technology.

References

[1]Lee, K. D., and Loellbach, J. M., "Geometry-Adaptive Surface Grid Generation Using a Parametric Projection," AIAA Paper 88-0522, Jan. 1988.

[2]Luh, R. C. C., "Surface Grid Generation for Complex Three-Dimensional Geometries," *Numerical Grid Generation in Computational Fluid Dynamics '88,* Pineridge, Swansea, England, 1988, pp. 85–94.

[3]Rao, V. C. V., Sundararajan, T., and Das, P. C., "A New Approach to Grid Generation Using Finite Element Technique," *Numerical Grid Generation in Computational Fluid Dynamics '88,* Pineridge, Swansea, England, 1988, pp. 157–166.

[4]Thompson, J. F., Warsi, Z. U. A., and Mastin, C. W., *Numerical Grid Generation: Foundations and Applications,* Elsevier, New York, 1985, Chap. 6.

[5]Murata, K., Oguni, T., and Karaki, Y., *Supercomputer Applications to Scientific Computation,* Maruzen, Tokyo, 1985 (in Japanese), pp. 141–149.

Similarity Solutions for Supersonic Axisymmetric Flows

Hamdi T. Hemdan*

King Saud University, Riyadh 11451, Saudi Arabia

Introduction

IT is well known that similarity solutions exist in several areas of gasdynamics, including unsteady one-dimensional and steady hypersonic flow past slender axisymmetric and two-dimensional bodies. For such bodies, Sedov[1] has shown that the solutions have power-law shock waves and negligible freestream pressure. His work was later reviewed by Mirels[2] with emphasis on hypersonic flow. Cole and Aroesty[3] have shown that, for two-dimensional flow, the hypersonic small disturbance theory (HSDT) permits another similarity solution with exponential shock waves.

Received Jan. 8, 1990; revision received Oct. 17, 1990; accepted for publication Oct. 23, 1990.

*Associate Professor, Mathematics Department.

Later, Hui[4] found another similarity solution with logarithmic shock waves for two-dimensional flow. Both solutions,[3,4] similar to that of Sedov, assumed infinite M_∞. To show the effect of finite values of M_∞, Hui and Hemdan[5] perturbed the two solutions[3,4] and reduced the perturbation equations to ordinary differential equations. Here, we give new similarity solutions based on a recently developed hypersonic theory given in Ref. 6.

Perturbation Theory

The problem of hypersonic flow past pointed-nose slender axisymmetric bodies at zero incidence was approximated[6] as follows:

$$\hat{p}_x + (\hat{p}v)_r + \hat{p}v/r = 0 \tag{1a}$$

$$n\hat{p}_r + \hat{p}(v_x + vv_r) = 0 \tag{1b}$$

$$v[x, F(x)] = F'(x) \tag{2}$$

$$\hat{p}[x, S(x)] = S'^2(x) \tag{3a}$$

$$v[x, S(x)] = S'(x) - n/S'(x) \tag{3b}$$

where

$$n = 1/[1 + (\gamma - 1)M_\infty^2/2]$$

γ is the ratio of the specific heats of the gas, and $\hat{p}$, v, F, and S are, respectively, nondimensional: pressure, transverse speed, body, and shock wave. The variables $\hat{p}$, v, and S are related to the physical values $\bar{p}$, $\bar{v}$, and $\bar{S}$ by the following perturbation expansion:

$$\bar{p}(\bar{x},\bar{r}) - P_\infty = \rho_\infty U_\infty^2[\epsilon\hat{p}(x,r) - \epsilon n) + O(\epsilon^2)] \tag{4b}$$

$$\bar{v}(\bar{x},\bar{r}) = U_\infty[\sqrt{\epsilon}v(x,r) + O(\epsilon^{3/2})] \tag{4b}$$

$$\bar{S}(\bar{x}) = l[\sqrt{\epsilon}S(x) + O(\epsilon^{3/2})] \tag{4c}$$

where x and r are the physical axial and radial coordinates (see Fig. 1); P_∞, ρ_∞, and U_∞ the freestream pressure, density, and speed; l the body length; and ϵ the perturbation parameter defined by

$$\epsilon = \frac{\gamma - 1}{\gamma + 1} + \frac{2}{(\gamma + 1)M_\infty^2} \tag{5}$$

Finally, x and r are nondimensional coordinates defined by

$$x = \bar{x}/l \tag{6a}$$

$$r = \bar{r}/l\sqrt{\epsilon} \tag{6b}$$

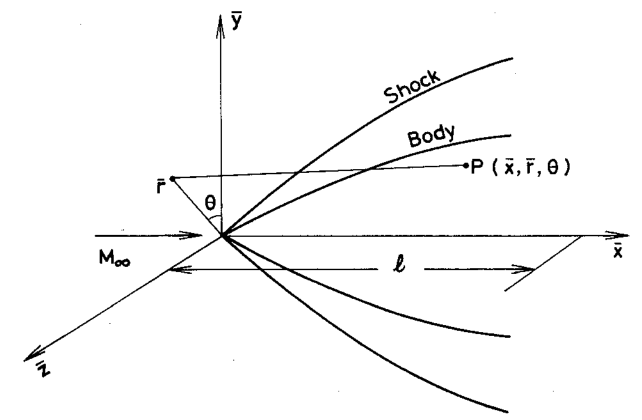

Fig. 1 Axisymmetric body and coordinates.

The motivation behind this approach and the main assumptions involved are detailed in Ref. 6 and could be summarized briefly as follows. It is well known that, should the limits $\gamma \to 1$ and $M_\infty \to \infty$ be applied to the full steady inviscid equations, we would get the Newtonian theory. To divert from the Newtonian approximation and to get equations applicable at hypersonic speeds, and possibly moderate speeds, the preceding limits are associated with a geometric limiting process in which the body thickness $\to 0$ as $\sqrt{\epsilon}$. Thus, Eqs. (1–3) are valid in the limits $\gamma \to 1$ and $M_\infty \to \infty$ and $\bar{F}(\bar{x}) \to 0$ with $(\gamma - 1)M_\infty^2$ and $\bar{F}(\bar{x})/\sqrt{\epsilon}$ fixed. Since $\epsilon < 1$ for supersonic flows, the theory could also be used at moderate Mach numers. Notice that M_∞ is $O(1/\sqrt{\epsilon})$ and the body thickness measured by say, δ, is $O(\sqrt{\epsilon})$; thus, it follows that the proper range of $M_\infty \delta$, the Tsien hypersonic parameter, is $O(1)$ or greater, similar to the HSDT.

Equations (1) may be simplified by the transformation

$$\tilde{p}(x,r) = \ln \hat{p}(x,r) \tag{7}$$

Now, we assume the following perturbation expansion as $k \to 0$.

$$v(x,r) = v_0(\eta) + kx^m v_1(\eta) + k^2x^{2m}v_2(\eta) + \ \ldots \tag{8a}$$

$$\tilde{p}(x,r) = p_0(\eta) + kx^m p_1(\eta) + k^2x^{2m}p_2(\eta) + \ \ldots \tag{8b}$$

$$F(x) = Bx - kx^{m+1} \tag{8c}$$

$$S(x) = Ax + akx^{m+1} + bk^2x^{2m+1} + \ \ldots \tag{8d}$$

where

$$\eta(x,r) = r/x$$

is the similarity parameter, and m is any number greater than 0, and B is the slope of some basic cone. The constants A, a, and b in Eq. (8d) are to be found as part of the solution, and the functions on the right-hand sides of Eqs. (8) are assumed to be $O(1)$ as $k \to 0$.

Substituting Eqs. (8) into Eqs. (2), (3b), and the transformed [by Eq. (7)] form of Eqs. (1) and (3a), and equating like powers of k, we obtain the following approximations:

Zero approximation:

$$(v_0 - \eta)\eta p_0' + \eta v_0' + v_0 = 0 \tag{9a}$$

$$np_0' + (v_0 - \eta)v_0' = 0 \tag{9b}$$

$$v_0(B) = B \tag{10}$$

$$v_0(A) = A - n/A \tag{11a}$$

$$p_0(A) = 2\ln A \tag{11b}$$

First approximation:

$$(v_0 - \eta)p_1' + v_1' + mp_1 + (p_0' + \frac{1}{\eta})v_1 = 0 \tag{12a}$$

$$np_1' + (v_0 - \eta)v_1' + (m + v_0')v_1 = 0 \tag{12b}$$

$$v_1(B) = v_0'(B) - m - 1 \tag{13}$$

$$v_1(A) = a(m+1)(1 + n/A^2) - av_0'(A) \tag{14a}$$

$$p_1(A) = 2a(m+1)/A - ap_0'(A) \tag{14b}$$

Second approximation:

$$(v_0 - \eta)p_2' + v_2' + 2mp_2 + (p_0' + \frac{1}{\eta})v_2 = -v_1p_1' \tag{15a}$$

$$np_2' + (v_0 - \eta)v_2' + (2m + v_0')v_2 = -v_1v_1' \tag{15b}$$

$$v_2(B) = v_1'(B) - \frac{1}{2}v_0''(B) \tag{16}$$

$$v_2(A) = b(1+2m)(1 + n/A^2) - na^2(1+m)^2/A^3$$
$$- av_1'(A) - bv_0'(A) - \tfrac{1}{2}a^2v_0''(A) \tag{17a}$$

$$p_2(A) = 2b(1+2m)/A - a^2(1+m))^2/A^2 - ap_1'(A)$$
$$- bp_0'(A) - \frac{1}{2}a^2p_0''(A) \tag{17b}$$

It should be mentioned that Jischke and Kim[7] have also studied the axisymmetric flow past slender bodies using the HSDT also by seeking the flow as a small perturbation from some basic cone flow. They obtained a first-order perturbation term that should correspond to the first approximation given earlier. They presented only one comparison for the surface pressure, which showed marked deviation from experiment and the tangent-cone method except for the leading part of the body.

Solutions for Axisymmetric Bodies

The pressure p_0 could be eliminated from Eqs. (9) to get

$$v_0' = -v_0 \Bigg/ \left\{ \eta \left[1 - \left(\frac{v_0 - \eta}{\sqrt{n}} \right)^2 \right] \right\} \tag{18}$$

Equation (18) is nonlinear and has two singular points corresponding to $v_0(\eta) - \eta \pm \sqrt{n} = 0$. Using Eqs. (10) and (11a), we can show that the numerator of Eq. (18) varies between $v_0(B)$ and $v_0(A)$ as η varies from A to B; therefore, it cannot be zero anywhere and the singular points are not in the flowfield. It can be shown that Eqs. (12) and (15) have the same singular points.

Equations (12–14) can be transformed into an initial-value problem by the transformation

$$P_1(\eta) = p_1(\eta)/b, \qquad V_1(\eta) = v_1(\eta)/b$$

Results and Comparison

The surface pressure coefficient, C_p, will be given by

$$C_p = -2n\epsilon + 2\epsilon \exp\{p_0(B) + kx^m[p_1(B) - p_0'(B)]$$
$$+ k^2x^{2m}[p_2(B) - p_1'(B) + \frac{1}{2}p_0''(B)]\} \tag{19}$$

The shock wave of a circular cone will be determined by A only, which can be found from Eq. (11a) (taking the weak shock solution).

Table 1 compares C_p for circular cones with semivertex angles θ_c with Sims'[8] numerical solution for $\gamma = 1.4$. The table shows that Eq. (19) is in very good agreement with Sims' exact calculations, even for M_∞ as low as 3 and θ_c as high as 20 deg.

In Fig. 2, the circular cone shock wave is compared with exact calculations ($A = \tan\theta_s\sqrt{\epsilon}$). The agreement is seen to be

Table 1 Comparison for C_p for circular cones

	$\theta_c = 10$ deg		$\theta_c = 15$ deg		$\theta_c = 20$ deg	
M_∞	Sims	Eq. (19)	Sims	Eq. (19)	Sims	Eq. (19)
20	0.0640	0.0632	0.1411	0.1449	0.2458	0.2664
15	0.0648	0.0640	0.1419	0.1455	0.2466	0.2671
10	0.0667	0.0659	0.1441	0.1476	0.2489	0.2693
7	0.0699	0.0690	0.1478	0.1514	0.2531	0.2732
5	0.0748	0.0734	0.1542	0.1572	0.2605	0.2800
4			0.1608	0.1630	0.2684	0.2799
3					0.2843	0.2798

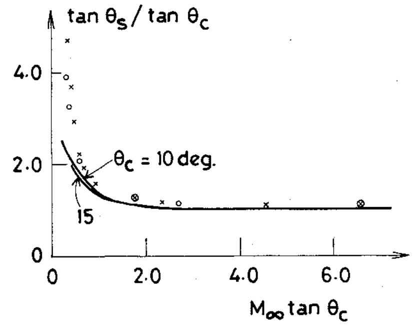

Fig. 2 Comparison for shock-wave angle θ_s for a cone: ○, × exact (○, 10 deg; ×, 15 deg); ——, Eq. (11a); $\gamma = 1.405$.

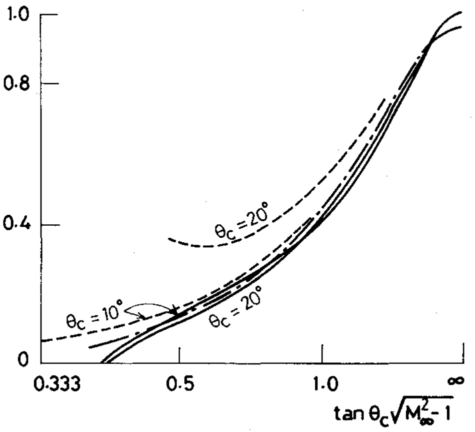

Fig. 3 Comparison for ratio of shock wave to body initial curvature ν for a parabolic ogive: - - -, exact; —–—, HSDT; ——, Eq. (8d); $\gamma = 1.405$.

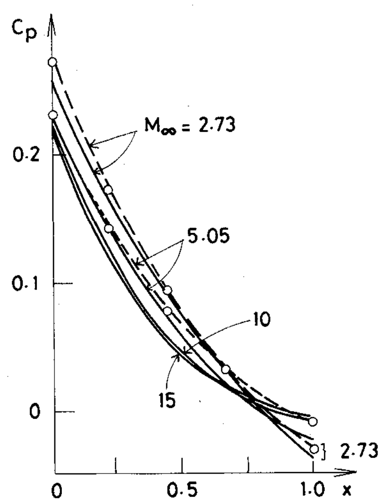

Fig. 4 Comparison for C_p on a parabolic ogive of fineness ratio 3: ○, experiment; - - -, method of characteristics; ——, Eq. (19); $\gamma = 1.405$.

good if $M_\infty \tan\theta_c$ is $O(1)$ or greater. In Fig. 3, the ratio of shock wave to body initial curvature, ν, is compared with exact calculations and with the HSDT for a class of ogives ($m = 1$ and $k = B/2$). The figure shows good agreement with the exact calculations for $\theta_c = 10$ deg.

Figure 4 compares Eq. (19) with experiment and the method of characteristics. Notice the good agreement even for $M_\infty = 2.73$. The figure also shows that increasing M_∞ has a moderate decreasing effect for the front part of the body and a moderate increasing effect on the very rear part.

Conclusions

Very good results are obtained for pointed-nose slender axisymmetric bodies at zero incidence. The agreement with the exact method and experiment covers a wide range of γ, M_∞, and k. The analysis relies on a recent formulation of the hypersonic small disturbance theory, where the equations have been reduced here to ordinary differential equations. The main advancement of the present hypersonic theory lies in having a smaller number of unknown functions and easier equations that lend themselves to further analytical study.

References

[1]Sedov, L. I., *Similarity and Dimensional Methods in Mechanics,* Academic, New York, 1959, Chap. 4, (English translation).

[2]Mirels, H., *Hypersonic Flow over Slender Bodies Associated with Power-Law Shocks,* Vol. 7, Advances in Applied Mechanics, 1962.

[3]Cole, J. D., and Aroesty, J., "Hypersoic Similarity Solutions for Airfoils Supporting Exponential Shock Waves," *AIAA Journal,* Vol. 8, 1970, pp. 308–315.

[4]Hui, W. H., "A Solution for Hypersonic Flow Past Slender Bodies," *Journal of Fluid Mechanics,* Vol. 48, Pt. 1, 1971, pp. 23–31.

[5]Hui, W. H., and Hemdan, H. T., "Higher Order Similarity Solutions for Hypersonic Flow Past Airfoils," *Proceedings of the International Conference on Symmetry, Similarity and Group Theoretic Methods in Mechanics,* Univ. of Calgary, Canada, May 1974, pp. 403–417.

[6]Hemdan, H. T., "Newtonian Flow over Axisymmetric Bodies," *Transactions of the Japan Society of Aeronautical and Space Sciences,* Vol. 32, No. 95, 1989, pp. 13–25.

[7]Jischke, M. C., and Kim, B. S., "Hypersonic Flow Past an Axisymmetric Body with Small Longitudinal Curvature," *AIAA Journal,* Vol. 20, No. 10, 1982, pp. 1346–1351.

[8]Sims, J. L., "Tables for Supersonic Flow Around Right Circular Cones at Zero Angles of Attack," NASA SP-3004, 1964.

Resonance Prediction for Slotted Circular Wind Tunnel Using Finite Element

In Lee* and Ki-Young Baik†

Korea Advanced Institute of Science and Technology, Daejon, Korea

Introduction

MODEL flutter and unsteady airload measurements will be affected by resonant phenomena. When the model frequency is near a wind-tunnel resonant frequency, the results of these test will be inaccurate. Widmayer et al.[1] conducted some experiments to measure the oscillatory aerodynamic forces and moments acting on a rectangular wing. The test results were in considerable error near the tunnel resonant frequency. Clevenson and Widmayer[2] also observed the occurrence of resonance in experiments on a two-dimensional wing. Therefore, it is important to predict the wind-tunnel resonant frequency accurately.

Davis and Moore[3] and Acum[4] have obtained the resonance frequencies for the rectangular cross section. Lee[5] has obtained the resonance frequencies for a rectangular and an octagonal cross section by using finite elements.

Some wind tunnels have circular cross sections. Also, many wind tunnels have several slots on the wall to reduce model

Received March 9, 1990; revision received Aug. 6, 1990; accepted for publication Aug. 21, 1990.

*Associate Professor, Department of Aerospace Engineering, 373-1, Kusung-dong, Yusung-ku. Member AIAA.

†Mechanical Engineer, Kia Motors Corporation.